

Impact of IBR Negative Sequence Current Characteristic on Distance Protection

Prashanth Kumar Mansani, Mohammad Zadeh
ETAP

Ilia Voloh
GE Renewable Energy

Originally presented at the
74th Georgia Tech Protective Relaying Virtual Conference, April 2021

Impact of IBR Negative Sequence Current Characteristic on Distance Protection

Prashanth Kumar Mansani, Mohammad Zadeh
ETAP
Irvine, CA, USA

Iliia Voloh
GE Renewable Energy
Markham, Canada

Abstract— Inverter-based resources (IBRs) may inject non-conventional or no negative-sequence current during unbalanced faults. Recent German Grid Code and latest draft of IEEE P2800 mandate injection of negative-sequence current (I_2) proportional to negative-sequence voltage (V_2) during unbalanced faults. Some vendors of Type III wind turbine generators prefer to inject I_2 leading V_2 by 135-150 degrees while synchronous generators inject I_2 leading V_2 in the range of 90-100 degrees. In this paper, the impact of different IBR negative-sequence current injection on fault type identification and impedance-based protection functions is studied. The response of the IBR is compared to a synchronous generator of the same rating. Simulation results are validated by injecting COMTRADE files to a commercial relay.

Keywords— Inverter; impedance protection, negative-sequence current injection

I. INTRODUCTION

Negative sequence current injection of inverter-based resources (IBRs) heavily depends on the control logic adopted by IBR manufacturers. Recent German Grid Code [1] and latest draft of IEEE P2800 mandate injection of I_2 proportional to V_2 during unbalanced faults [2]. In case of synchronous generator, I_2 typically leads V_2 by 90° to 100° . This is the desired angle range to ensure that existing protection functions are not adversely impacted. IBRs may inject no negative sequence current, unconventional negative sequence current and the one that is similar to synchronous machines. Several WTG Type III vendors also prefer to inject I_2 leading V_2 by the angle range of 135° to 150° . This paper will investigate the impact of such fault current characteristics on impedance-based protection functions including fault type identification adopted by major relay vendors.

Fault type identification is used in distance protection function to enable faulted loops and block un-faulted loops. Same or different fault type identification logic may be used for alarming, recording, single-pole tripping and fault location that is not studied in this paper. This paper just focuses on fault type identification logic used as part of the core distance protection function. Phase angle between I_2 and I_0 is dependent on the fault type and relay vendors utilize the phase angle relationship along with other techniques to identify the fault type. In this paper, fault type identification algorithms employed by two major relay vendors are simulated and the impact of IBRs on the algorithms is investigated using ETAP software. Software

generated COMTRADE files are injected to commercial relays to validate the simulation results.

Relay vendors utilize phase comparators and/or impedance-based methods to implement impedance-based protection functions. The impact of IBR with no or proper negative sequence current injection on different implementation of distance functions was studied by authors in [3], [4]. In this paper, the impact of IBR negative-sequence current injection specially the preferred case of wind turbine Type III will be investigated on different impedance-based protection functions adopted by major relay vendors. Test system parameters have been updated based on field data and the software generated COMTRADE files will be injected to commercial relays to validate simulation results.

II. FRT REQUIREMENTS

As the penetration of IBRs increased, IBRs have been mandated to follow fault-ride-through (FRT) requirements to resolve possible reliability concerns. So modern-day inverters dynamically support positive-sequence voltage (DPS) of the system by increasing positive-sequence current injection during voltage drop defined by a K factor, i.e., the slope of the fault-ride-through curve ($\Delta I / \Delta V$) of the IBR. K is usually chosen between 2 and 7. IBR may prioritize reactive power injection and curtail real power injection depending on the control mode.

German code updated in 2017 mandates IBRs to inject both positive and negative sequence currents during the fault. There is a growing awareness in the power system community in North America for the IBRs to dynamically support positive and negative-sequence voltage during unbalanced faults (DPNS). In DPNS, positive and negative-sequence sequence current are injected as per (1) and (2).

$$I_{q1} = -jK_1 \times \Delta V_1 = -jK_1 \times |V_{1\text{fault}} - V_{1\text{pre-fault}}| \quad (1)$$

$$I_{q2} = jK_2 \times \Delta V_2 = jK_2 \times |V_{2\text{fault}} - V_{2\text{pre-fault}}| \quad (2)$$

Injecting only positive-sequence voltage may result in over-voltage issues in healthy phases, and non-homogeneity as presented in [3], [4]. The impact of IBR fault current characteristics on source-impedance-ratio (SIR) is discussed in Section IV. To better analysis the impact of IBR on SIR, first a test system is introduced in the following section.

III. TEST SYSTEM PARAMETERS

A test system of 100 MW capacity is simulated in ETAP by aggregating 50 IBRs with 2 MW capacity each. IBRs are connected to the grid through a Yg-D unit transformer and Yg-Yg-D plant transformer and 93.2-mile-long transmission line as shown in Fig. 1. The response of IBR is compared to an alternate system where the IBR is replaced by a synchronous generator of the same capacity. In this investigation, steady state short circuit is performed and transient behavior of IBRs immediately after fault is ignored. This approach is justified as the adverse impact is mostly on fault locations that are close to the end of the line. These faults fall within Zone 2 of distance protection that is time delayed.

Aggregated IBR is first assumed to be connected to a strong point of the grid, so the modeled IBR is connected to a grid with SIR of 0.17 modeled as a voltage source behind a constant impedance. As the renewable energy penetration increases in future, most of the renewable stations will be connected to a weak grid. To simulate this scenario, an alternate system is created where the IBR is connected to a weak grid with SIR of 6.23. The K factor is set to 5 for positive-sequence and 5.9 for negative-sequence injection. As a result, the fault response of the IBR will be like a conventional generator with sub-transient reactance of 20 % and negative-sequence reactance of 17 %.

Three different scenarios are simulated based on the fault characteristics of the inverter as shown below.

1. Conventional IBRs with dynamic positive sequence injection (DPS).
2. Modern IBRs with dynamic positive and negative sequence injection. I_2 leading V_2 by 90° , similar to synchronous generator, is injected in this scenario (DPNS Con).
3. IBRs with dynamic positive and negative sequence injection. Several WTG Type III vendors inject I_2 leading V_2 by about 135° - 150° . Therefore, in this scenario I_2 leads V_2 by 150° (DPNS Non-Con).

IV. THE IMPACT OF IBR ON SIR

Most IBR's are typically designed to output no more than 120 to 150% of their rated power for a few seconds. Hence, lines interconnected to IBR source will be a high SIR. To better quantify the level of SIR, it is important to understand IBR fault current characteristics. Conventional generators act as a voltage source behind an impedance; however, IBRs connected to a transmission system operated in grid following mode act as a controlled current source within the inverter capacity. Further, the fault current characteristic is mandated by grid codes including fault ride through capability as well as reactive power injection proportional, typically linear, to the voltage drop [1].

For a linear FRT reactive current injection as explained earlier, the fault characteristics of the inverter will be similar to a synchronous generator with $1/K_1$ positive and $1/K_2$ negative sequence reactance within the IBR short circuit limit. However, if the inverter reaches the short circuit limit, fault current contribution will be limited. In this region, equivalent source impedance changes with the fault voltage as the fault current is

maintained constant. Therefore, depending on the fault location, the behavior of the inverter changes.

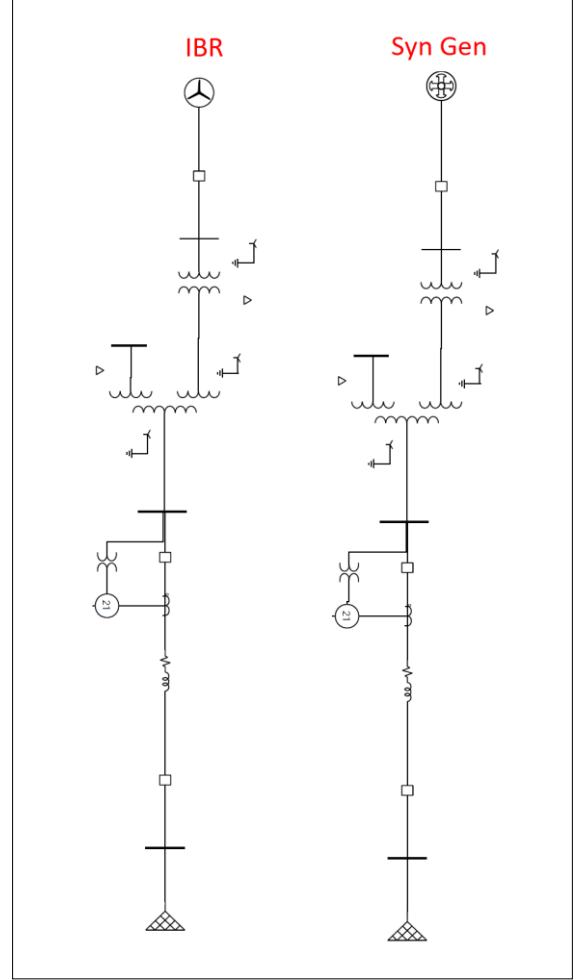


Fig. 1 One-line diagram

To study the impact of IBR on SIR, different fault types are inserted along the line and the SIR is calculated as shown below [5].

$$SIR_{3PH} = (V_{Base} - V) / (I \times Z_1) \quad (3)$$

$$SIR_{LG} = (V_{Base} - V) / ((I + I_0 K_0) \times Z_1) \quad (4)$$

where V is the phase voltage, I is the phase current, I_0 is the zero-sequence current, Z_1 is the positive-sequence impedance of the line and K_0 is the zero-sequence compensation factor given by $Z_0/Z_1 - 1$. Fig. 2 shows the SIR for 3-ph close-in and remote faults. It can be observed that SIR of the IBR is almost twice of the generator. As a result, generator causes almost twice the voltage measured by the relay as shown in Fig. 2.

Table 2 shows the SIR at the relay for single-phase fault, it can be observed that the SIR for the IBR with negative-sequence injection is close to the generator. However, for IBR with DPS, the SIR is approximately 15% higher than the generator resulting in 11 % more voltage measured by the relay. This study shows that even though IBR short circuit capacity is significantly limited, i.e., 350% in this case as compared to a

synchronous generator, its SIR is only 53% less in the worst cases of bolted three phase faults.

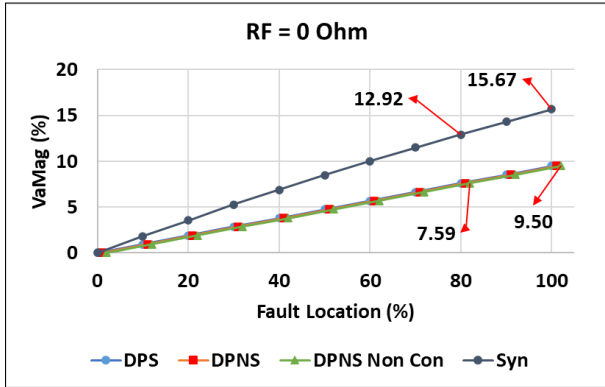


Fig. 2 Phase voltage for 3ph-fault
Table 1. SIR for 3-phase fault

Source	$\angle I_2 - \angle V_2$	Fault Location (%)	SIR
Syn Gen	-	0	5.42
IBR DPS	-	0	10.55
IBR DPNS Con	90°	0	10.55
IBR DPNS Non-con	150°	0	10.55
Syn Gen	-	100	5.47
IBR DPS	-	100	9.56
IBR DPNS Con	90°	100	9.56
IBR DPNS Non-con	150°	100	9.56

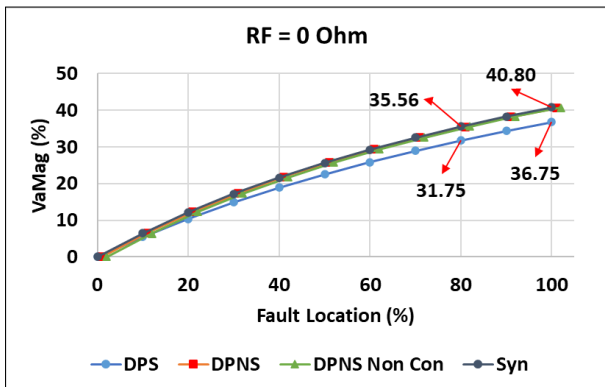


Fig. 3 Phase voltage for LG fault

In a conventional synchronous generator-based plant, positive, negative and zero sequence equivalent source impedances seen from the interconnecting line local terminal have the similar or at least consistent characteristic angle compared to the remote end equivalent source. IBRs on the other hand may inject non-conventional or no negative-sequence current during unbalanced faults. This results in non-conventional negative sequence source impedance and non-homogenous system. The non-homogeneity creates an angle difference between the current measured by the relay and fault current. The angle difference may adversely impact line relay performance if relay is not properly set.

To study the impact of IBR on the level of non-homogeneity, line-to-ground faults are inserted at various fault locations along the line with the fault resistance of 0 ohm. The

impact of fault location on the non-homogeneity can be observed from Fig. 4, where ΔI_{Ang} is the angle difference of the faulted phase current ($\angle I_{IBR(A)} - \angle I_{Grid(A)}$). It can be observed that phase angle difference for synchronous generator is almost constant irrespective of fault location. As IBRs with DPS operates within the SC limit during fault therefore IBR behaves like a generator with $1/K_1$ sequence impedance and phase angle difference is constant. As IBRs with DPNS Con, and DPNS Non-Con inject both positive and negative sequence currents to support faulted phase voltage, they hit the short-circuit limit for close faults. As a result, phase angle difference between sending and receiving end changes based on the fault location leading to an uncertain non-homogeneity.

Table 2. SIR for LG fault

Source	$\angle I_2 - \angle V_2$	Fault Location (%)	SIR
Syn Gen	-	0	1.45
IBR DPS	-	0	1.72
IBR DPNS Con	90°	0	1.43
IBR DPNS Non-con	150°	0	1.49
Syn Gen	-	100	1.45
IBR DPS	-	100	1.72
IBR DPNS Con	90°	100	1.47
IBR DPNS Non-con	150°	100	1.46

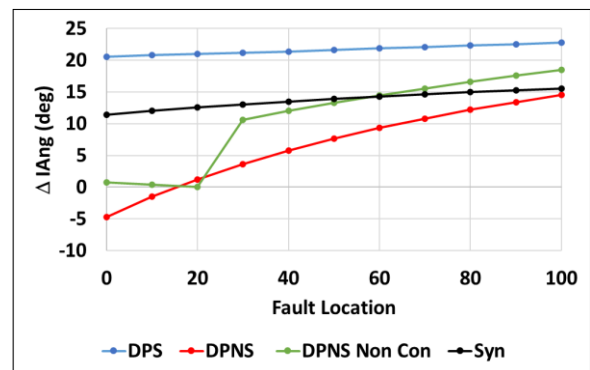


Fig. 4 Impact of IBR on non-homogeneity for LG fault

V. FAULT TYPE IDENTIFICATION

Fault-loops are generally categorized into six, three ground loops (AG, BG, CG) and three phase loops (AB, BC, and CA) to cover all fault types. Distance function directly or indirectly estimates fault loop impedance, i.e., the positive sequence impedance between relay location and fault location, in each loop and compare it against the setting value. However, multiple fault loops can be triggered for a single fault due to system conditions [6], therefore fault type identification algorithms are used to detect the fault type and enable respective loops. Several fault type identification algorithms have been developed and employed by the relay vendors. However, the impact of IBR on two popular algorithms are studied in this paper. Each of the algorithms is briefly discussed in the following.

1) *Algorithm I*: In this method [7], phase angle difference between negative sequence and zero sequence current as given by (5) to determine the faulted loop.

$$\text{AngleDiff} = \angle I_2 - \angle I_0 \quad (5)$$

Each sector is assigned fault types based on experimental analysis as described below:

1. Sector 1: If AngleDiff falls between $+30^\circ$ and -30° , the fault could be either AG or BCG fault. Fault resistance is calculated for both the loops (AG and BC) and the loop with the lowest value is selected as faulted loop.
2. Sector 2: If AngleDiff falls between -90° and -150° , the fault could be either BG or CAG fault. Fault resistance is calculated for both the loops and the loop with the lowest value is selected as faulted loop.
3. Sector 3: If AngleDiff falls between 90° and 150° , the fault could be either CG or ABG fault. Fault resistance is calculated for both the loops and the loop with the lowest value is selected as faulted loop.
4. Sector 4: If AngleDiff falls between 30° and 60° or -30° and -60° . Here, the fault is determined in two steps
 - a. Calculate the reach for AB, BC and CA loops and select the loop with the lowest reach.
 - b. Compare the fault resistance of the selected loop and AG loop to determine the fault.
5. Sector 4: If AngleDiff falls between -60° and -90° or -150° and -180° . Here, the fault is determined in two steps
 - a. Calculate the reach for AB, BC and CA loops and select the loop with the lowest reach.
 - b. Compare the fault resistance of the selected loop and BG loop to determine the fault.
6. Sector 4: If AngleDiff falls between 60° and 90° or 150° and 180° . Here, the fault is determined in two steps
 - a. Calculate the reach for AB, BC and CA loops and select the loop with the lowest reach.
 - b. Compare the fault resistance of the selected loop and CG loop to determine the fault.

2) *Algorithm II*: This algorithm [8], can be described as follows:

1. Ground loops are activated if,
 - a. $\text{AngleDiff} < 50^\circ$.
2. Phase loops are activated if
 - a. The fault is not SLG, where SLG refers to one of the phase voltages satisfy $|V_{\text{Ph1}} + V_0| < 0.98|V_{\text{Ph2-Ph3}}|/\sqrt{3}$ and the other two phases do not satisfy the same.
 - b. I_0, I_2 are present and greater than threshold then
 - i. AB loop is activated if $|\text{AngleDiff} + 120^\circ| < 70^\circ$.
 - ii. CA loop is activated if $|\text{AngleDiff} + 240^\circ| < 70^\circ$.

iii. BC loop is activated if $|\text{AngleDiff}| < 70^\circ$.

- c. At least two of the phase voltages are below 85 % of the nominal voltage.

If unconventional negative-sequence current is injected into the system, AngleDiff can become greater than 50° and this algorithm fails to detect the fault accurately. For IBR with DPS, these algorithms are bypassed as there is no negative-sequence current.

VI. DISTANCE PROTECTION

Distance protection compares the estimated impedance between the relay and fault location against a setting characteristic to determine the fault. Modern distance relays can be classified based on impedance-based protection function into 1- phase-comparator and 2- impedance measurement-based method. The operation of each method and impact of IBR fault current characteristics on each method is briefly discussed in the following.

A. Phase-comparator-based Method

Phase-comparators compare the phase angle difference between polarizing and operating phasor signals to determine the fault. Mho, Quadrilateral characteristics can be created by the using a one or combination of several phase comparators [5][9].

Mho characteristic is a circle used to determine phase-to-ground as well as phase-to-phase faults. Positive-sequence memory voltage is widely used as a polarizing signal to prevent mal-operation during close-in faults. This results in dynamic expansion of mho characteristic depending on the change in voltage angle during the fault. IBRs without negative sequence injection utilize full converter capacity to support the positive-sequence voltage, therefore change in voltage angle is smaller relative to the IBRs with negative-sequence injection. This results in larger dynamic expansion in case of IBRs with negative-sequence injection.

Quadrilateral characteristics are usually employed for detecting phase-to-ground fault. Phase comparators are used to compare 1- Reactance, 2 – Reverse reactance, 3 – Right blinder, 4 – Left blinder against the settings value to determine the fault. The polarizing signal of reactance comparator is formed using either phase current or zero-sequence current, or negative-sequence current. Negative-sequence current is a popular choice in modern relays as negative-sequence networks are more homogeneous. However, lack of negative-sequence current from IBRs results in mal-operation of relays utilizing negative-sequence current for polarization.

B. Impedance-Measurement (IM)-based Methods

IM-based methods estimate impedance or a combination of resistance and reactance and compare against a user-specified characteristic to determine the fault. IM-based methods used by major relay vendors can be broadly classified into four types. Method IV is a combination of phase comparator and Method III, therefore discussion of the impact of IBR on this method is omitted in this paper. Table 3 shows the equations used in each

method. Details on how each equation is derived was presented by authors in [4][5].

Method I and Method II utilize phase current to estimate the fault loop impedance, thus these methods are not directly impacted by the IBRs. However, depending on the relay vendors, Method-III may use 1) $3I_0$, 2) $1.5 \times I_0 + 1.5 \times I_2$, and 3) $3I_2$ to estimate I_F for LG fault. For LL faults, negative-sequence current is used for calculating the compensating current ($I_{comp} = j\sqrt{3} I_2$). Therefore, based on the choice of fault current, this method can be significantly impacted by the fault characteristics of the IBR.

Table 3. Impedance-Measurement-based Methods

Method I	$mZ_1 = V_a / (I_a + K_0 I_0)$
Method II	$mX_1 = \frac{Im\{V_a\} Re\{I_R\} - Re\{V_a\} Im\{I_R\}}{Re\{I_X\} Re\{I_R\} + Im\{I_X\} Im\{I_R\}}$
	$R_{seen} = \frac{Im\{V_a\} Im\{I_X\} + Re\{V_a\} Re\{I_X\}}{Re\{I_X\} Re\{I_R\} + Im\{I_X\} Im\{I_R\}}$
Method III (LG)	$mX_1 = Im\{V_a \times I_F^*\} / Im\{(R_1/X_1 + j)(I_a + K_0 I_0) I_F^*\}$
	$R_F = Im\{V_a(Z_1^*(I_a + K_0 I_0)^*)\} / Im\{I_F(Z_1^*(I_a + K_0 I_0)^*)\}$
	$R_{seen} = mR_1 + R_F = (mX_1) \times (R_1/X_1) + R_F$
Method III (LL)	$mX_1 = Im\{V_{bc} \times I_{comp}^*\} / Im\{(R_1/X_1 + j)I_{bc} I_{comp}^*\}$
	$0.5R_F = Im\{V_{bc}(Z_1 I_{bc})^*\} / Im\{2 I_{comp}(Z_1 I_{bc})^*\}$

VII. SIMULATION AND TESTING RESULTS

In this section, the impact of DPS and DPNS on fault type identification and distance protection is discussed in detail for both phase-to-ground and phase-to-phase fault loops.

A. Fault type identification

Fault type identification algorithms utilize phase angle relationship between zero-sequence and negative-sequence current to determine the fault as discussed in the earlier section. Therefore, to study the impact of IBR with DPNS, two scenarios corresponding to low impedance and high impedance fault conditions are simulated with various phase angle of I_2 with respect to V_2 . From Table 1, Algorithm-I correctly detects the fault in all conditions. Algorithm-II detects the fault when $\angle I_2^\circ - \angle V_2^\circ$ is below 150° , however at 180° the algorithm doesn't detect the fault as LG. Considering that the I_2 angle range leading V_2 reported by WTG type 3 vendors is less than 150° degree, both algorithms are expected to perform correctly.

Table 4. Fault type identification results for AG faults

$\angle I_2 - \angle V_2$	Fault Location (%)	R _F	Fault Type	Algorithm I	Algorithm II
90°	5	1	AG	AG	AG, BC
90°	50	12	AG	AG	AG, BC
135°	5	1	AG	AG	AG, BC
135°	50	12	AG	AG	AG, BC
150°	5	1	AG	AG	AG, BC
150°	50	12	AG	AG	AG, BC
175°	5	1	AG	AG	AG, BC
175°	50	12	AG	AG	AG, BC
180°	5	1	AG	AG	Non-AG, AB, BC
180°	50	12	AG	AG	AG, BC

For algorithm II, to validate simulation results, COMTRADE files were generated for the case of phase-to-ground fault type and low impedance fault resistance and played back as an input to the corresponding commercial relay. From Table 6, it can be concluded that Algorithm II operated as per simulation results.

Table 5. Fault type identification results for BCG faults

$\angle I_2 - \angle V_2$	Fault Location (%)	R _F	Fault Type	Algorithm I	Algorithm II
90°	5	1	BCG	BCG	MPH, AG
90°	50	12	BCG	BCG	MPH, AG
135°	5	1	BCG	BCG	MPH, AG
135°	50	12	BCG	BCG	MPH, AG
150°	5	1	BCG	BCG	MPH, AG
150°	50	12	BCG	BCG	MPH, AG
175°	5	1	BCG	BCG	MPH
175°	50	12	BCG	BCG	MPH, AG
180°	5	1	BCG	BCG	MPH
180°	50	12	BCG	BCG	MPH, AG

Table 6. Actual relay playback results to test Algorithm II

$\angle I_2 - \angle V_2$	Fault Location (%)	R _F	Fault Type	Hardware Results	Simulation Results
150°	5	1	AG	AG	AG
180°	5	1	AG	Non-AG	Non-AG

B. Distance protection

1) Phase-to-ground loop

In this section, the impact of IBRs on phase-comparator based methods and IM-based methods is discussed for phase-to-ground faults.

a) Phase-comparator-based method

Mho characteristics expand dynamically based on the system strength during a fault. As short-circuit capacity of synchronous generator is higher than the IBR, dynamic expansion is smaller in synchronous generator compared to IBR with DPNS.

In a strong system, the change in the voltage angle is small. As a result, the resistive coverage of synchronous generator and IBR is almost similar as shown in Fig. 5. In weak system, the change in voltage angle is significant. Therefore, as shown in Fig. 6, the resistive coverage is smaller in synchronous generator compared to IBR with DPNS as discussed earlier. The response of phase comparator is not significantly impacted by different IBR negative-sequence current injection. Also, resistive coverage of IBR with DPS is less than DPNS as it uses full converter rating to support positive-sequence voltage as discussed in Section IV. COMTRADE files are played back into a commercial mho relay to validate simulation results for the case of strong grid. From Table 7, it can be inferred that the resistive reach of the relay is between 12 and 18 ohms. Therefore, hardware results match simulation results.

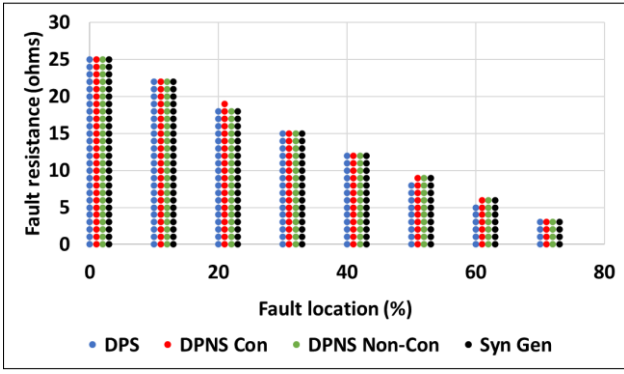


Fig. 5 Expected trip for LG fault in a strong system

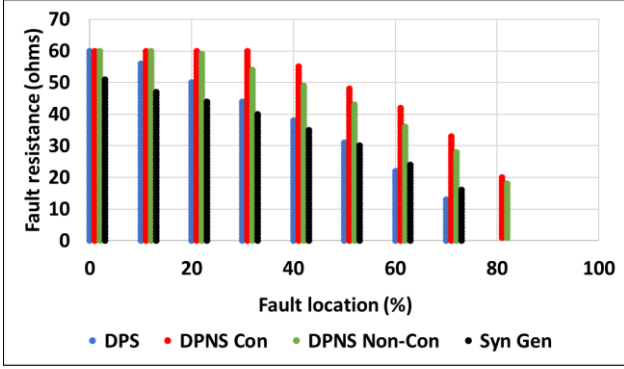


Fig. 6 Expected trip for LG fault in a weak system

Table 7. Actual relay playback results to test mho relay for LG fault

Source	Fault Location (%)	R_F	Hardware Results	Simulation Results
IBR DPS	30	12	Trip	Trip
IBR DPS	30	18	No trip	No trip
IBR DPNS Con	30	12	Trip	Trip
IBR DPNS Con	30	18	No trip	No trip
IBR DPNS Non-con	30	12	Trip	Trip
IBR DPNS Non-con	30	18	No trip	No trip
Syn Gen	30	12	Trip	Trip
Syn Gen	30	18	No trip	No trip

b) Impedance-Measurement-based(IM-based) Methods

To study the impact of IBR, estimated impedances for Methods I to III are compared with the actual fault impedance as shown below,

$$\Delta R_{\text{seen}} = R_{\text{seen}} - R_F \quad (6)$$

$$\Delta X_{\text{seen}} = X_{\text{seen}} - X_F \quad (7)$$

where, R_{seen} and X_{seen} correspond to the resistance seen, reactance seen by the line relay at the IBR side and R_F , X_F represent the actual fault resistance and loop reactance, respectively.

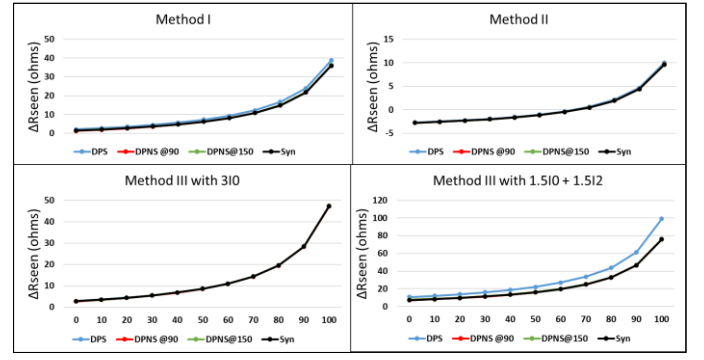


Fig. 7 ΔR_{seen} for LG fault in a strong system at $R_f = 5$ ohms

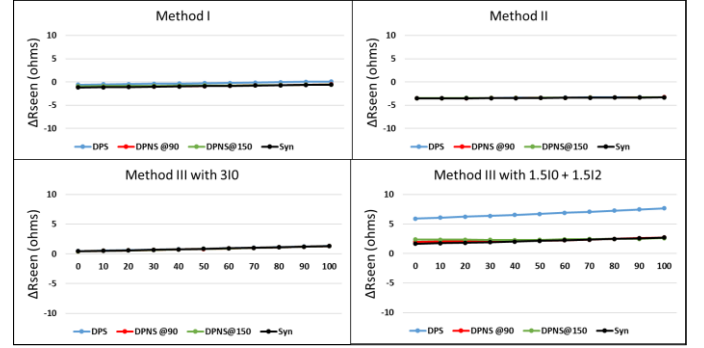


Fig. 8 ΔR_{seen} for LG fault in a weak system at $R_f = 5$ ohms

Simulation results for the error in seen resistance are shown in Fig. 7 and Fig. 8. For strong system, Method I and Method II are not considerably affected. Method III with $3 \times I_0$ as I_F is not impacted, however with $(1.5 \times I_0 + 1.5 \times I_2)$ as I_F is significantly impacted. Lack of negative sequence current (DPS) results in higher seen resistance error, phase angle of IBR negative-sequence current does not significantly impact the estimated resistance. As infeed is smaller in weak system error in overall seen resistance is considerably smaller as compared to a strong system.

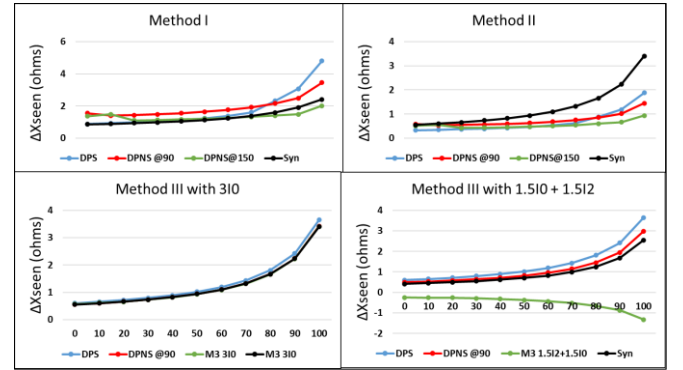


Fig. 9 ΔX_{seen} for LG fault in a strong system at $R_f = 5$ ohms

The impact of IBR on the estimated reactance for strong and weak systems is shown in Fig. 9 and Fig. 10, respectively. It can be inferred that lack of or improper negative-sequence injection does not have any considerable adverse impact on the seen reactance estimation even for the case where IBR is connected to a strong system with considerable infeed.

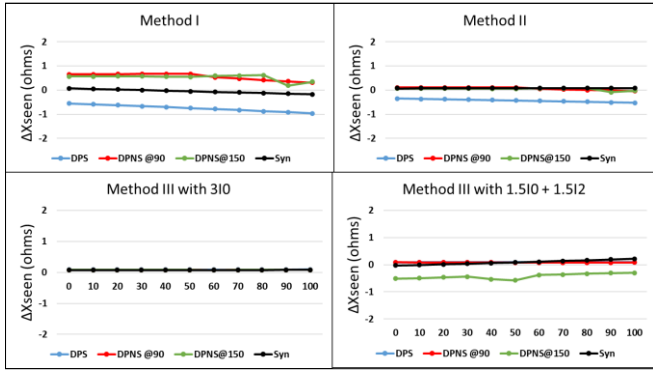


Fig. 10 ΔX_{seen} for LG fault in a weak system at $R_f = 5$ ohms

2) Phase-to-phase loop

The impact of IBRs on phase-to-phase fault loop for phase comparator-based and Method III is discussed in the following section.

a) Phase-comparator-based method

Dynamic expansion of mho characteristic can result in increased resistive coverage for LL faults similar to LG faults. In strong systems as shown in Fig. 11, change in voltage angle is small, therefore increase in resistive coverage is small for DPNS with conventional I_2 compared to DPS. The response of phase comparator is not significantly impacted by injecting non-conventional I_2 . In weak systems, the change in voltage angle results in increased resistive coverage as shown in Fig. 12.

b) Impedance-Measurement-based (IM-based) Methods:

This method directly employs negative sequence current for impedance estimation as given by Table 3. As this method gives incorrect results for DPS, corresponding discussion is omitted in the results. Expected trip results for DPNS are provided in Fig. 13 - Fig. 14 with resistive reach setting as 20 ohms. It can be observed that, resistive reach is reduced by infeed from the grid. As the infeed is higher in strong systems, resistive coverage is adversely impacted. In weak systems, the impact on relay performance is smaller because of smaller infeed. As this method utilize magnitude of negative-sequence current for impedance estimation, there are no significant differences between conventional and non-conventional negative sequence current.

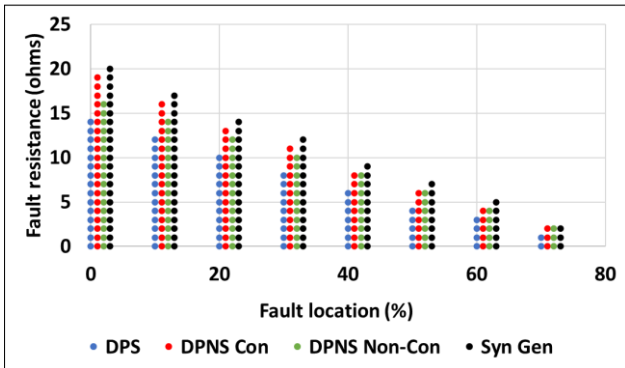


Fig. 11 Expected trip for LL fault in a strong system

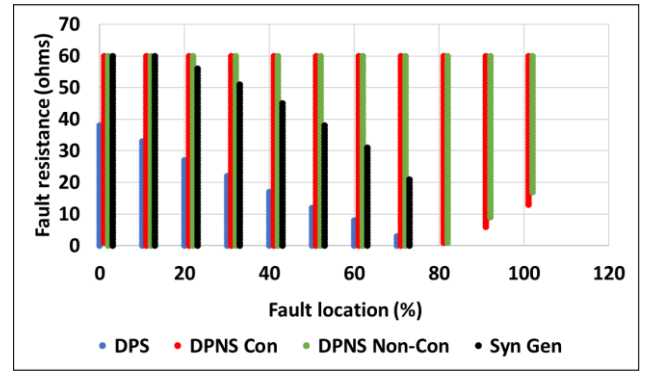


Fig. 12 Expected trip for LL fault in a weak system.

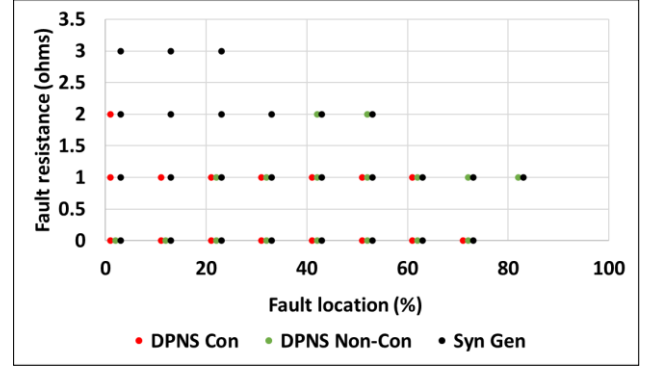


Fig. 13 Expected trip for LL fault in a strong system

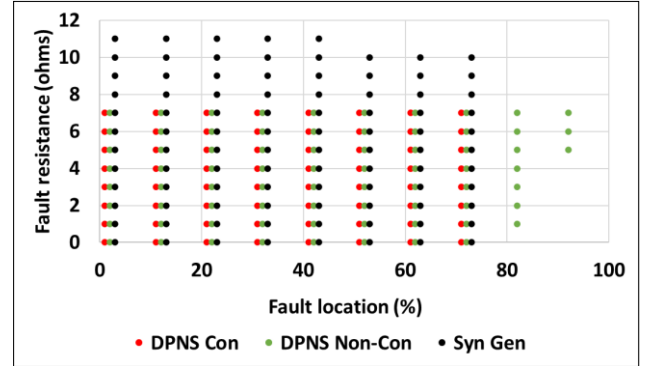


Fig. 14 Expected trip for LL fault in weak system

VIII. CONCLUSION

Fault current characteristics of IBR is studied with positive sequence current injection, conventional and non-conventional negative sequence current. It is concluded that IBR acts as a controlled current source with varying impedance, as a result the effect of non-homogeneity cannot be estimated accurately. In addition, IBRs with DPNS reach short circuit capacity more frequently as they support faulted phases by injecting both positive and negative sequence current.

Fault type identification logic algorithms employed by at least two relay vendors is studied for low impedance and high impedance faults. It is concluded that Algorithm I is unaffected by the angle of negative-sequence current for LG and LLG faults. Algorithm II failed to detect the LG fault at $\angle I_2^\circ$ leading $\angle V_2^\circ$ by 180° , however this does not fall in the normal operation range of the inverter and the algorithm correctly detected the LLG fault. Therefore, it can be concluded that the

fault type identification output is not significantly affected when the $\angle I_2^\circ$ is below 150° .

Phase comparator-based methods are not significantly affected for LG fault. In impedance-measurement based methods, Method I and Method II are not affected by the unconventional negative-sequence current. It is concluded that, error in Method III employing $(1.5 \times I_0 + 1.5 \times I_2)$ is higher when IBRs doesn't inject negative-sequence current. For line-line fault, unconventional negative-sequence current marginally impacts the resistive coverage. Method III impedance-measurement based relays are not significantly affected by phase angle of I_2 .

REFERENCES

- [1] "Summary of the draft VDE-AR-N 4120," May 2017.
- [2] A. Rajapakse, R. Majumder, S. G. R. Energy and R. Nelson, "Modification of commercial fault calculation programs for wind turbine generators," 2020. [Online]. Available: https://www.pes-psrc.org/kb/published/reports/C24_WG_Report_Jun_2020_Final.pdf
- [3] M.R.D Zadeh, M. P. Kumar, and D. Ting, "Impact of inverter-based resources on impedance-based protection functions," in Proc. Developments in Power System Protection, Liverpool, UK, Mar 9-12, 2020.
- [4] M. R. D. Zadeh, M. P. Kumar, and I. Voloh, "Impact of inverter-based resources on impedance-based protection functions," in Proc. 46th Western Protective Relay Conference, Oct 19-22, 2020.
- [5] M. J. Thompson and A. Somani, "A tutorial on calculating source impedance ratios for determining line length," in Proc. 68th Annual Conf. for Protective Relay Engineers, pp. 833-841 Mar 2015.
- [6] E.O. Schweitzer III, and J. Roberts, "Distance relay element design," in Proc. 46th Annual Conf. for Protective Relay Engineers, College Station, TX. 1993.
- [7] D. Costello, and K. Zimmerman, "Determining the faulted phase," in Proc. 63rd Annual Conf. for Protective Relay Engineers, pp 1-20, Mar. 2010.
- [8] *D60 Line Distance Relay, Instruction Manual*, GE, 2020.
- [9] D. D. Fentie, "Understanding the dynamic mho distance characteristic," in Proc. 69th Annual Conf. for Protective Relay Engineers, College Station, Texas, USA, pp. 1-15, April, 2016.
- [10] US Federal Energy Regulatory Commission. "Standard interconnection agreement for wind energy," Docket No. RM05-4-000 (2005).